33RD INTERNATIONAL COSMIC RAY CONFERENCE, RIO DE JANEIRO 2013
THE ASTROPARTICLE PHYSICS CONFERENCE

ICRC 2013

Study of the time-dependence of the cosmic-ray anisotropy with AMANDA and IceCube

THE ICECUBE COLLABORATION[1],

[1] *See special section in these proceedings*

santander@icecube.wisc.edu

Abstract: The IceCube neutrino observatory and its predecessor, the AMANDA neutrino telescope, search for sources of astrophysical neutrinos against a high background of down-going muons originating from cosmic ray interactions in the atmosphere. The arrival direction of cosmic-ray muons is correlated with the direction of the original primary particle to within a degree for primary energies above several TeV. The large muon sample collected by both detectors provides us with a unique opportunity to study the arrival direction anisotropy of TeV cosmic rays in the southern sky over a time period of more than 12 years. A variation in the observed structure of the TeV anisotropy with time could provide hints about its origin. We present a search for time variability of the anisotropy observed by AMANDA between 2000 and 2006, and by IceCube between 2007 and 2012.

Corresponding authors: P. Desiati[1], M. Gurtner[2], K.-H. Kampert[2], T. Karg[2,a], M. Santander[1], S. Westerhoff[1]
[1] Wisconsin IceCube Particle Astrophysics Center, University of Wisconsin, Madison, WI 53706, U.S.A.
[2] Dept. of Physics, University of Wuppertal, D-42119 Wuppertal, Germany
[a] now at DESY, D-15735 Zeuthen, Germany

Keywords: Cosmic rays, Anisotropy, AMANDA, IceCube.

1 Introduction

Cosmic rays (CRs) in our galaxy are believed to originate in supernova remnants (SNRs) that can potentially accelerate charged particles up to PeV energies. The trajectories of these charged particles are affected by the presence of the magnetic field that permeates the galaxy. Cosmic rays propagating through the interstellar medium would scatter off of turbulences in the galactic magnetic field, which isotropizes their directions of arrival at Earth. This diffusion process creates gradients in the density of cosmic rays in the solar vicinity, which in turn should produce an anisotropy with a characteristic dipolar shape and a small amplitude of per-mille strength or lower (see [1] and references therein).

A number of experiments in the northern hemisphere have observed anisotropy at TeV energies (see [2] and others). The observed anisotropic structure in the sky shows two major features: an almost dipolar large angular scale component with a relative amplitude of $\sim 10^{-3}$ and several localized excess regions with typical sizes between 10° and 30° and relative amplitudes of $\sim 10^{-4}$. A similar structure has been observed in the southern sky using data from the IceCube detector [3, 4] at energies of about 20 TeV.

While it is possible that the large scale anisotropy is due to cosmic ray diffusion from nearby sources, its shape could be affected by the interaction of these cosmic rays with the heliosphere. It is known that cosmic rays with energies below 10 GeV are modulated by solar activity, but this influence should be less significant at higher energies. At primary energies of several TeV, the gyroradius of a proton in the μG-strength field of our galaxy is about 10^{-3} pc, which corresponds to scales of $\mathcal{O}(10^2)$ AU, similar to the size of the heliosphere. It has been argued [5] that given the similarity in these scales, it is possible that some of the observed structure in the anisotropy is due to scattering of cosmic rays in the heliosphere. Possible evidence for such a heliospheric influence on the anisotropy would be the observation of a variation in the anisotropy shape with the 11-year solar cycle. On much longer times scales (over thousands of years or more) a variation in the orientation and amplitude of the anisotropy is also expected due to changes in the cosmic-ray flux due to nearby sources [6].

Studies of the stability of the TeV anisotropy as a function of time have been performed by the Tibet [7], and Milagro [8] collaborations. While Tibet observes no significant variation in the anisotropy for the time period 11/1999 to 12/2008, Milagro reports a steady increase in the amplitude of the deficit region over a similar period of seven years (from 07/2000 to 07/2007). These stability studies can be extended to the southern hemisphere by analyzing the combined cosmic ray data set collected by the AMANDA and IceCube neutrino telescopes over the course of 12 years (from 2000 through 2011). Both detectors observe muons that originate in cosmic ray showers at very high rates, which has allowed us to collect multi-billion event data sets of cosmic ray muons with an angular resolution of a few degrees. The stable data taking conditions and the good angular resolution of both detectors make this study possible. The results of this search are presented in this work.

2 Detectors

2.1 AMANDA

AMANDA (Antarctic Muon And Neutrino Detector Array) [9] is the predecessor to the IceCube neutrino telescope. It consists of a three-dimensional array of 655 optical modules deployed over a volume of 3×10^{-3} km^3 at depths between 1500 m and 2000 m in the Antarctic ice sheet at the geographic South Pole. Optical modules are connected to 19 vertical cables, or "strings", that provide mechanical support, electrical power, and a data connection to the

surface. The final configuration of the detector, AMANDA-II, operated from 2000 to 2006. AMANDA is located at a similar depth below the ice surface as IceCube, making it sensitive to TeV muons from cosmic-ray air showers.

The median energy of the cosmic-ray primary particles that produce muons detected in AMANDA is about 10 TeV [11]. Cosmic-ray muons are considered background for most neutrino searches, so only minimal information is stored for these events. In this work, we use this minimal data to search for large-scale anisotropies in the arrival directions of cosmic rays.

2.2 IceCube

The IceCube neutrino telescope [10] is based on the same design principle as AMANDA. In IceCube, a total of 5160 Digital Optical Modules (DOMs), attached to 86 strings, are deployed over a volume of about 1 km^3 at depths between 1450 m and 2450 m below the ice surface.

Similarly to the AMANDA case, only limited information is stored for cosmic-ray muons events. The median energy of this limited cosmic ray sample is determined from simulations to correspond to about 20 TeV.

3 Data selection

3.1 AMANDA

For this analysis, we use AMANDA events that satisfy the M24 trigger condition. This trigger requires a light signal in ≥ 24 optical modules during a time window of 2.1 μs. For downward going muons from cosmic ray air showers, this corresponds to an energy threshold of a few hundred GeV, depending on the zenith angle. The data rate of the M24 trigger is approximately 100 Hz and follows seasonal variations in the atmospheric profile. The `DirectWalk` reconstruction algorithm [12], which has an angular resolution of about 4.8° [13], is applied online to all triggered events,. After reconstruction quality cuts, the data rate is reduced to approximately 60 Hz.

Maintenance, calibration procedures, and interferences from other experiments at South Pole can induce instabilities in the AMANDA data rate. To ensure that only data acquired under stable conditions are analyzed we exclude periods of unusually high or low rates. The data are divided in 5 minute long time slices and the event rate in each time slice is compared to the average event rate of the past 12 hours. Time slices in which the event rate deviates by more than 50% from the average rate are discarded.

3.2 IceCube

The main event trigger in IceCube is a simple multiplicity trigger called SMT8 that requires coincident hits in eight DOMs within 5 μs. For each trigger, all hits detected in coincidence by nearby DOMs within a $\pm 10\mu$s window are recorded and overlapping windows are merged. The SMT8 trigger rate shows a seasonal variation of $\pm 10\%$ over the course of a year, due to the change of atmospheric conditions that affect the muon production in air showers. The average trigger rate has increased over the years with the deployment of more strings in the ice, and is about 2700 Hz for the final 86-string configuration.

A first guess of the event direction is obtained by performing a linear-track fit to the DOM hits using an analytical χ^2 minimization procedure. The result of the linear fit is used as a seed to a more complex likelihood-based reconstruction that takes into account some aspects of the light generation and propagation in the ice. A single-iteration of this likelihood fit (with an angular resolution of about 3°) is run online at the South Pole and the corresponding information is later transmitted over satellite.

Similarly to AMANDA, only periods where the detector data rate was stable are taken into account.

4 Analysis method and results

The search for anisotropy is conducted by searching for deviations of the sky map of reconstructed cosmic ray arrival directions in equatorial coordinates from a reference isotropic sky map obtained from data using the time-scrambling method described in [14]. The time scrambling period used in the analysis is 24 hours, which makes it sensitive to all angular scales in the celestial sphere. During the time scrambling procedure, events were resampled 20 times to reduce statistical fluctuations in the reference sky map.

The sky maps were constructed using the HEALPix[1] library [15] that provides an equal area pixelization of the sphere. The chosen HEALPix resolution divides the sphere into 49152 pixels, with an average distance between pixel centers of approximately 1°.

Using the reference and data maps, a relative intensity map can be calculated using the expression $\delta I_i = (N_i - \langle N \rangle_i)/\langle N \rangle_i$, where N_i and $\langle N \rangle_i$ are, respectively, the number of observed events and the number of reference events for the isotropic expectation in the i^{th} pixel obtained with the time scrambling technique.

Maps are subjected to a smoothing procedure to increase the sensitivity of the anisotropy search to structures larger than the map pixel size. The smoothing process creates a map of correlated pixels where the number of events in each pixel corresponds to the integrated number of events in a circular region around that pixel. The radius of the circular region (i.e. the smoothing radius) defines the angular scale of the structure for which the sensitivity of the smoothing procedure is optimized. For the maps shown in Fig. 1, a smoothing radius of 20° was chosen.

As can be seen in Fig. 1, the anisotropy maps show significant large-scale structure of per-mille amplitude in the southern sky as already reported by IceCube [3]. At first glance, the anisotropy shape appears to be stable across the twelve periods of approximately one year each considered in this work.

In order to obtain a quantitative result, we compared the observed anisotropy profile from each period defined according to Table 1 to the global twelve-year average. For this exercise, one-dimensional projections of the anisotropy maps were obtained by binning the right ascension coordinate α in 15 statistically-independent intervals. The relative intensity $\delta I(\alpha)$ in the j^{th} right-ascension bin is calculated from the number of events in the data and reference maps contained in the declination range $-85° < \delta < -35°$.

The agreement between each yearly profile δI_y and the global average $\langle \delta I \rangle$ is estimated by a χ^2-test using the following expression:

$$\chi^2_y = \sum_{j=1}^{j=15} \frac{(\delta I_y(\alpha_j) - \langle \delta I(\alpha_j) \rangle)^2}{\sigma^2_{\delta I} + \sigma^2_{\langle \delta I \rangle}} , \qquad (1)$$

1. http://healpix.jpl.nasa.gov

Period	Detector	Start	End	Live-time (days)	No. of events ($\times 10^9$)	χ^2/dof	p-value
1	AM-II	02/13/2000	11/02/2000	213.4	1.4	11.3/15	0.73
2	AM-II	02/11/2001	10/19/2001	235.3	2.3	16.6/15	0.34
3	AM-II	01/01/2002	08/02/2002	169.2	2.4	26.0/15	0.04
4	AM-II	02/09/2003	12/17/2003	236.0	2.2	19.3/15	0.20
5	AM-II	01/05/2004	11/02/2004	225.8	2.5	14.3/15	0.50
6	AM-II	12/30/2004	12/23/2005	242.9	2.6	21.0/15	0.14
7	AM-II	01/01/2006	09/13/2006	213.1	2.4	24.4/15	0.06
8	IC22	06/01/2007	03/30/2008	269.4	5.3	45.2/15	7×10^{-5}
9	IC40	04/18/2008	04/30/2009	335.6	18.9	12.8/15	0.62
10	IC59	05/20/2009	05/30/2010	335.0	33.8	11.1/15	0.75
11	IC79	05/31/2010	05/12/2011	299.7	39.1	6.5/15	0.97
12	IC86	05/13/2011	05/14/2012	332.9	52.9	8.9/15	0.88

Table 1: Definition of each time period used in this analysis. AMANDA data sets are indicated as "AM-II", while IceCube data sets are marked as "IC" followed by the number of active detector strings during that time period. The number of live-days and recorded events is shown. Each time period is compared to the global twelve-year average using a χ^2-test. The χ^2 and the associated p-value for each period is also listed.

where the statistical uncertainties in each bin are calculated according to the expression:

$$\sigma_{\delta I} = \frac{N_j}{\langle N \rangle_j} \sqrt{\frac{1}{N_j} + \frac{1}{s\langle N \rangle_j}} \,. \quad (2)$$

Here, $s = 20$ is the number of resamples that was used in the calculation of the reference map. The combined uncertainty in the difference is obtained by adding the individual uncertainties in δI_y and $\langle \delta I \rangle$ in quadrature. The global uncertainty in each bin is dominated by the uncertainty in each yearly period due to the relatively lower level of statistics. Only statistical uncertainties have been considered so far. A future analysis will account for systematic effects that may be caused by the incomplete time coverage of each period which could lead to distortions in the right ascension profile (for instance, due to interference of the solar dipole anisotropy with the anisotropy in equatorial coordinates [4]).

A p-value was calculated for each reduced χ^2 value. A list of p-values is given in Table 1. With the exception of Period 8, all p-values show a good agreement between individual periods and the global average, given the statistical uncertainties of each set. The large p-values for periods 11 and 12 are expected since the large relative size of both data sets makes them dominate the global average profile. Period 8 corresponds to the start of regular operation of IceCube, where the detector operated with 22 active strings (about one quarter of the final size of the detector). Due to gaps in the data taking process and fluctuations in the muon rate, it is possible that the discrepancy is related to detector effects. The impact of these effects is currently under investigation.

A preliminary study of the amplitudes and phases of a first and second harmonic fit to the relative intensity profiles shows no significant modulation over time.

5 Conclusions

A study of the stability of the TeV cosmic ray anisotropy over a period of twelve years is presented using data recorded with the AMANDA and IceCube detectors. No significant time variation in the observed anisotropy is found with the exception of the period corresponding to the 22-string configuration of IceCube.

Since IC22 was the first year of regular operation of IceCube, instabilities in the detector configuration were common, which may have led to distortions in the observed anisotropy. Further stability studies are required to estimate the impact of these detector effects.

References

[1] P. Blasi and E. Amato, J. Cosmol. Astropart. Phys. 1/011 (2012) 11 doi:10.1088/1475-7516/2012/01/011.
[2] M. Amenomori et al., Science 314 (2006) 439 doi:10.1126/science.1131702.
[3] R. Abbasi et al., Astrophys. J. 718 (2010) L194 doi:10.1088/2041-8205/718/2/L194.
[4] R. Abbasi et al., Astrophys. J. 740 (2011) L16 doi:10.1088/0004-637X/740/1/16.
[5] P. Desiati and A. Lazarian, Astrophys. J. 762 (2013) 44 doi:10.1088/0004-637X/762/1/44.
[6] M. Pohl and D. Eichler, Astrophys. J. 766 (2013) 4 doi:10.1088/0004-637X/766/1/4.
[7] M. Amenomori et al., Astrophys. J. 711 (2010) 119 doi:10.1088/0004-637X/711/1/119.
[8] A. A. Abdo et al., Astrophys. J. 698 (2009) 2121 doi:10.1088/0004-637X/698/2/2121.
[9] E. Andres et al., Astropart. Phys. 13 (2000) 1 doi:10.1016/S0927-6505(99)00092-4.
[10] A. Achterberg et al., Astropart. Phys. 26 (2006) 155 doi:10.1016/j.astropartphys.2006.06.007.
[11] D. A. Chirkin, PhD thesis (2003) University of California, Berkeley.
[12] J. Ahrens et al., Nucl. Instrum. Meth. A524 (2004) 169 doi:10.1016/j.nima.2004.01.065.
[13] P. Steffen, Tech. Report AMANDA-IR/20010801, DESY, 2001.
[14] D. E. Alexandreas et al., Nucl. Instr. Meth. A328 (1993) 570 doi:10.1016/0168-9002(93)90677-A.
[15] K. M. Gorski et al., Astrophys. J. 622 (2005) 759 doi:10.1086/427976.

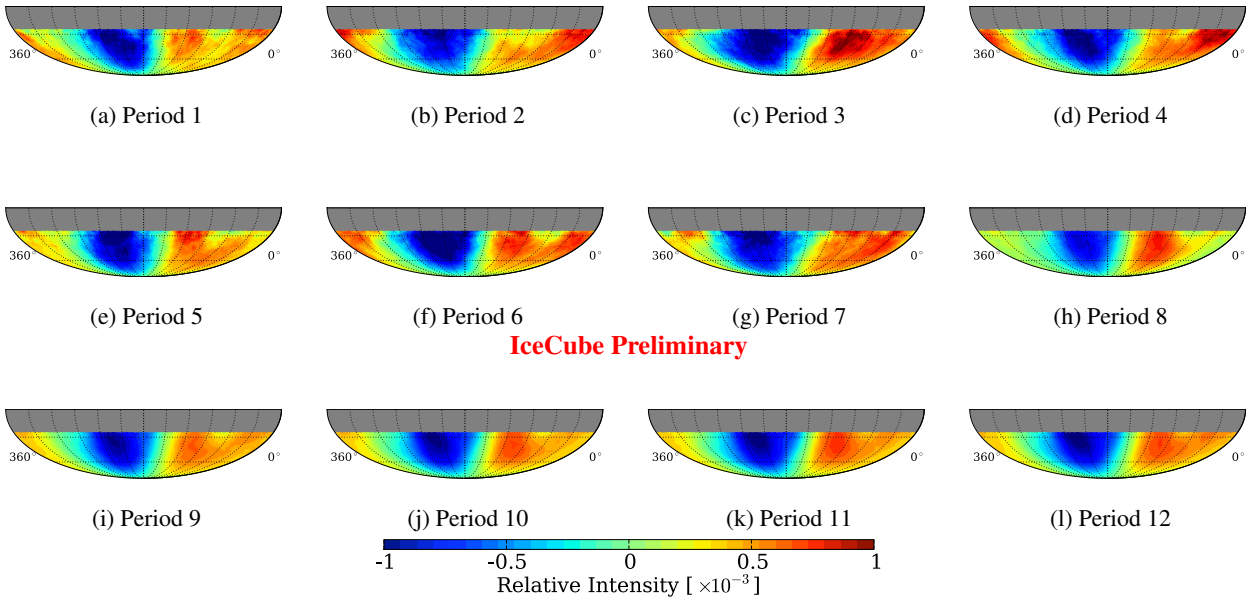

Figure 1: Two-dimensional relative intensity maps in equatorial coordinates of the cosmic ray anisotropy for the 12 time periods covering the years from 2000 to 2012 (see Table 1). All maps have been smoothed using a circular window with a 20° angular radius.

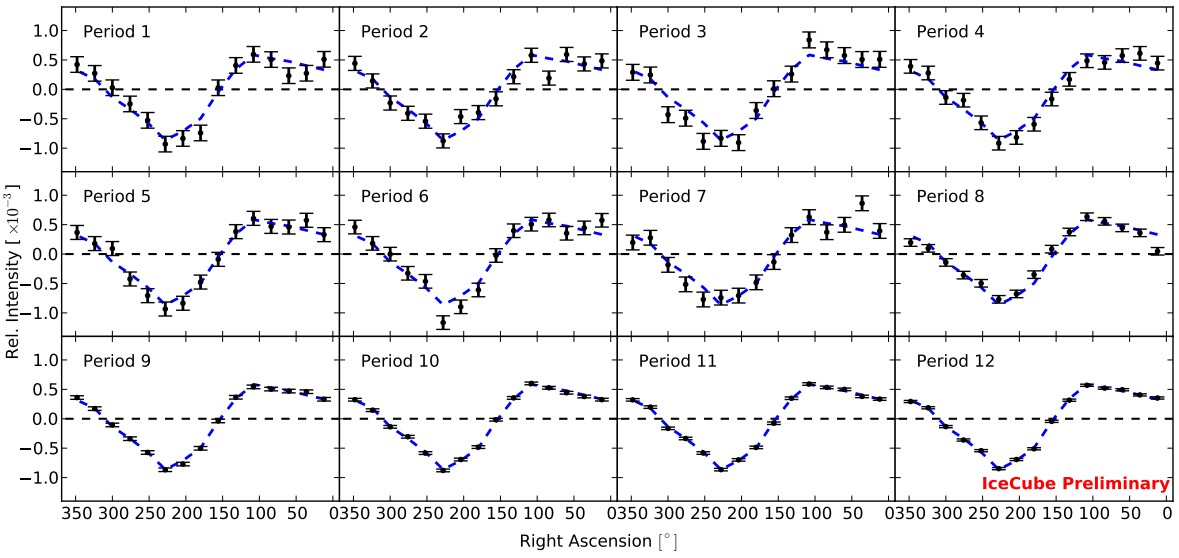

Figure 2: One-dimensional projections of relative intensity as a function of right ascension for the 12 time periods considered in this work. As a reference, the average profile for the entire data set is shown as a dashed blue line. The uncertainties shown are only statistical.